

Plant-derived natural polyphenols as potential antiviral drugs against SARS-CoV-2 via RNA-dependent RNA polymerase (RdRp) inhibition: An *in-silico* analysis

Satyam Singh¹, Avinash Sonawane¹, Sushabhan Sadhukhan^{2*}

¹Discipline of Biosciences and Biomedical Engineering, Indian Institute of Technology Indore, Simrol, Madhya Pradesh 453 552, India. ²Discipline of Chemistry, Indian Institute of Technology Palakkad, Kerala 678 557, India

*Corresponding author. *E-mail address:* sushabhan@iitpkd.ac.in (S. Sadhukhan).

Abstract: The sudden outburst of Coronavirus disease (COVID-19) has left the entire world to a standstill. COVID-19 is caused by Severe Acute Respiratory Syndrome Coronavirus 2 (SARS-CoV-2). As per the report from the WHO, more than 4.5 million people have been infected by SARS-CoV-2 with more than 3,00,000 deaths across the globe. As of now, there is no therapeutic drug or vaccine approved for the treatment of SARS-CoV-2 infection. Hence, the outbreak of COVID-19 poses a massive threat to humans. Due to the time taking process of new drug design and development, drug repurposing might be the only viable solution to tackle COVID-19. RNA-dependent RNA polymerase (RdRp) catalyzes SARS-CoV-2 RNA replication, *i.e.* the synthesis of single-stranded RNA genomes, an absolutely necessary step for the survival and growth of the virus. Thus, RdRp is an obvious target for antiviral drug design. Interestingly, several plant-derived polyphenols have been shown to inhibit enzymatic activities of RdRp of various RNA viruses including polio-virus type 1, parainfluenza virus type 3, and respiratory syncytial virus etc. More importantly, natural polyphenols have been used as a dietary supplementation for humans for a long time and played a beneficial role in immune homeostasis. Therefore, we were curious to study the binding of dietary polyphenols with RdRp of SARS-CoV-2 and assess their potential as an effective therapy for COVID-19. In this present work, we made a library of twenty potent polyphenols that have shown substantial therapeutic effects against various diseases. The polyphenols were successfully docked in the catalytic pocket of RdRp of SARS-CoV and SARS-CoV-2, and detailed studies on ADME prediction, toxicity prediction and target analysis were performed. The study reveals that EGCG, quercetagenin, and myricetin strongly bind to the active site of SARS-CoV-2 RdRp. Our studies suggest that EGCG, quercetagenin, and myricetin can inhibit RdRp and represent an effective therapy for COVID-19.

Keywords: SARS-CoV-2; RNA-dependent RNA polymerase (RdRp); Docking studies; Natural polyphenols; EGCG; Quercetagenin; Myricetin.

1. Introduction

An outbreak of Coronavirus disease (COVID-19) has caused a pandemic situation across the globe. Although the outburst was first observed at Wuhan city in China, at present more than 200 countries and territories around the world have witnessed the COVID-19 fatalities affecting all age groups. As of May 15, 2020, more than 4.5 million people have been affected by the disease, with a fatality of 3,04,963 across the globe as per the WHO report. Unfortunately, there is no clinically approved drug or vaccine for COVID-19 as of now. The disease is caused by the Severe Acute Respiratory Syndrome Coronavirus 2 (SARS-CoV-2), a member of the Coronaviridae family of viruses and it belongs to the same family *Betacoronaviruses*, like severe acute respiratory syndrome (SARS) and Middle East respiratory syndrome (MERS) (1,2). The symptoms of SARS-CoV-2 infection include fever, dry cough, shortness of breath, runny nose and sore throat (3). SARS-CoV-2 is a positive-sense single-stranded RNA virus and its genome is around 29.7 kB long with twelve putative open reading frames (ORFs) that encode different viral structural and non-structural proteins. There are four structural proteins in SARS-CoV-2, namely spike (S), envelope (E), membrane (M), and nucleocapsid (N), and all of them can potentially serve as an antigen for neutralizing antibody preparation as potential therapeutics.

Another, potential drug target for SARS-CoV-2 is RNA-dependent RNA polymerase (RdRp) which is a key component of the replication machinery of the virus to make multiple copies of the RNA genome. RdRp in various coronaviruses are remarkably similar. For example, the RdRp of SARS-CoV exhibits ~97% sequence similarity with that of SARS-CoV-2. More importantly, there is no human polymerase counterpart that resembles the sequence/structural homology with RdRp from coronaviruses, and hence, the development of RdRp inhibitors could be a potential therapeutic strategy without risk of crosstalk with human polymerases (4,5). Very recently, Yin et al. reported the crystal structure RdRp of SARS-CoV-2 complexed with an antiviral drug, Remdesivir highlighting how the template-primer RNA is recognized by the polymerase enzyme and the chain elongation is inhibited by Remdesivir providing a basis for developing a wide range of effective inhibitors to overcome from SARS-CoV-2 infection (6). RdRp has been found to be an effective drug target for several RNA viruses, spanning from the hepatitis C virus, zika virus to coronaviruses (7-9). The active site of RdRp is highly conserved and the catalytic domains contain two consecutive aspartate residues in a beta-turn joining $\beta 15$ and $\beta 16$ (10). The general structure

of RdRp consists of 7 motifs (A to G) among them inner channel of catalytic sites represented by motif A to C and they play a crucial role during the nucleotide addition cycle (11,12).

Epidemiological studies repeatedly suggested that consumption of bioactive compounds (e.g. vitamins, phytochemicals, polyphenols, flavonoids, flavonols, and carotenoids) has beneficial activity on human health and could minimize the risk of various diseases starting from cancers to viral infections (13). Traditional natural compounds have been consumed since ancient times as they exhibit less toxicity, low-cost availability, minimum side-effects and are rich in therapeutic resources. Some of the previous findings also suggest that naturally occurring compounds possess a wide range of antiviral properties against RNA viruses including polio-virus type 1, parainfluenza virus type 3, and respiratory syncytial virus by inhibiting their replication (14). In that context, Ahmed-Belkacem et al. have screened more than forty potent natural flavonoids for their polymerase inhibition activity using HCV-NS5 strain and among the different flavonoids, quercetagenin showed strong HCV replication inhibitory activity *in vitro* (15). Previously, song et al. reported that green tea catechins, by disrupting the membrane of the influenza virus, inhibited neuraminidase in the crude system (16). On a separate report, Takashi et al. reported that EGCG, a green tea polyphenol can inhibit the endonuclease activity of influenza A virus RNA polymerase. EGCG is also reported to interfere with viral replication *via* modulating the cellular redox environment (17,18). Therefore, the existing scientific evidence strongly suggests that natural flavonoids/polyphenol can act against a variety of RNA viruses. Because of the time-consuming process of new synthetic/semi-synthetic drug development, drug repurposing of phytomolecules is an ideal alternative in this urgent situation as the latter process is economical and scalable in a very short period of time. Hence, a comprehensive understanding of their binding to SARS-CoV-2 RdRp can yield interesting findings that can further be capitalized to develop COVID-19 drugs. Nevertheless, the apparent lack of cytotoxicity of polyphenols at even significantly high concentrations makes them potential antiviral drug candidates. In the present study, we selected twenty natural polyphenols with reported or predicted binding affinity towards RdRp of different RNA viruses. The selected library was then explored to assess the binding affinity of individual polyphenols towards RdRp of SARS-CoV and SARS-CoV-2 by molecular docking. Among the selected polyphenols, EGCG, myricetin, and quercetagenin were found to be successfully docked in the active site of RdRp of both SARS-CoV and SARS-CoV-2 with a highly favourable

affinity for the binding pocket. Remdesivir and GTP (a physiological nucleotide) were taken as positive controls to validate our results.

2. Methods

2.1 Molecular docking studies

2.1.1 Protein preparations. The crystal structures of SARS-CoV RdRp (PDB ID: 6NUR) (19) and SARS-CoV-2 RdRp (PDB ID: 6M71) (20) were retrieved from the protein databank (www.rcsb.org) (21). All the crystal structures were prepared individually by adding hydrogen atoms and computing Gasteiger charge using the AutoDock v4.2 program (22). The same process was repeated for both the proteins and subsequently saved as .pdbqt format in preparation for molecular docking.

2.1.2 Ligand preparations. The SDF structures of GTP, remdesivir, apigenin, baicalein, tricetin, luteolin, robinetin, fisetin, morin, datiscetin, 5-deoxygalangin, gossypetin, catechin, genistein, EGCG, curcumin, kaempferol, isorhamnetin, myricetin, galangin, quercetin and quercetagenin were retrieved from the PubChem database (<https://pubchem.ncbi.nlm.nih.gov/>) (23). The compounds were converted into pdb format and conformational energies of all the compounds were minimized by using UCSF Chimera (24).

2.1.3 Docking studies using AutoDock Vina. The energy-minimized structure of all the natural polyphenols, remdesivir, and GTP were docked with the receptor (RdRp of SARS-CoV and SARS-CoV-2) using AutoDock Vina 1.1.2 (25). The ligand files were further saved in PDBQT file format, a modified pdb format containing atomic charges, atom type definitions for ligands, and topological information (rotatable bonds). A grid box (30 Å × 30 Å × 30 Å) centered at (143, 143, 151) Å and (121, 120, 125) Å for the SARS-CoV RdRp, SARS-CoV-2 RdRp respectively, was used in the docking experiments. After the receptor-ligand preparation, docking runs were started from the command prompt. The lowest binding energy and best-docked conformation were considered as the ligand molecule with maximum binding affinity.

2.1.4 Protein-ligand interactions. LigPlot⁺ was used to investigate protein-ligand interactions for a given .pdb file containing the docked conformation (26). The LigPlot⁺

program self-generated schematic 2D representations of protein-ligand interaction. The output file represents the intermolecular interactions and their strengths, including hydrogen bonds, hydrophobic contacts, and atom accessibilities. H-bonds are shown in green dotted lines whereas residues involved in hydrophobic interaction are represented in red semicircle.

2.2 ADMET studies

The toxicity profile of remdesivir, EGCG, myricetin, and quercetagenin were predicted based on their ADMET profile. The ADMET studies (absorption, distribution, metabolism, elimination, and toxicity) were predicted using the pkCSM tool (<http://biosig.unimelb.edu.au/pkcsm/prediction>) (27). The canonical SMILE molecular structures of the above-mentioned compounds were retrieved from the PubChem database (www.pubchem.ncbi.nlm.nih.gov).

2.3 Molecular target prediction

Natural compounds interact with a large number of proteins, enzymes, lipids. This interaction plays a crucial role in elucidating the molecular mechanism of the small molecules. So, it is important to identify the molecular targets for new molecules (28). Swiss Target Prediction website (<http://www.swisstargetprediction.ch/index.php>) was logged on and canonical SMILE molecular structures of remdesivir, EGCG, myricetin and quercetagenin were entered in the search bar option and results were analyzed.

3. Results and discussion

3.1 Molecular docking analysis

3.1.1 The binding mode analysis and predicted binding affinity calculations of natural polyphenols against the SARS-CoV RdRp. Molecular docking has become a reliable drug discovery tool for selecting the potential lead compounds against a target protein. The docking score provides the binding affinity and type of interactions between the drug and target. The lower the value of the binding energy, the higher would be the efficacy of the drug. We investigated twenty selected natural polyphenols (structure and their sources are given in **Table S1** in the Supplementary Information) for their potential binding to the catalytic pocket of SARS-CoV RdRp (PDB ID: 6NUR) using molecular docking (**Table 1**). Docking results, based on binding energy value (ΔG) of the top five natural polyphenols are

mentioned in **Table 2**. Guanosine-5'-triphosphate (GTP), a physiologically relevant nucleotide exhibited ΔG of -8.2 kcal/mol for SARS-CoV RdRp. Remdesivir was taken in our study as a positive control as it is known to bind RdRp of SARS-CoV and SARS-CoV-2 (29,30). Remdesivir displayed the lowest binding energy -8.3 kcal/mol to RdRp of SARS-CoV. Five natural polyphenols among the twenty selected ones exhibited significantly high binding affinity towards SARS-CoV RdRp with ΔG for EGCG, myricetin, robinetin, quercetagenin, and isorhamnetin being -8.2, -8.1, -7.9, -7.8, -7.8 kcal/mol respectively (see **Table 2**). These five natural polyphenols were found to efficiently bind to the active site of SARS-CoV RdRp and hence, can be anticipated to block the polymerase activity of RdRp.

Table 1. Binding energy (kcal/mol) of the natural polyphenols along with control compounds against RdRp of SARS-CoV (PDB ID: 6NUR) and SARS-CoV-2 (PDB ID: 6M71)

S. No.	Compound name	Binding energy (kcal/mol)	
		Against SARS-CoV RdRp	Against SARS-CoV-2 RdRp
1.	GTP	-8.2	-7.9
2.	Quercetagenin	-7.8	-6.9
3.	Quercetin	-7.7	-6.9
4.	Galangin	-7	-6.3
5.	Myricetin	-8.1	-7.2
6.	Isorhamnetin	-7.8	-6.7
7.	Kaempferol	-7.5	-6.7
8.	Curcumin	-7.3	-6.9
9.	EGCG	-8.2	-7.3
10.	Genistein	-7.1	-6.1
11.	Catechin	-7.4	-6.2
12.	Gossypetin	-7.7	-6.6
13.	5-Deoxygalangin	-7.6	-6.7
14.	Datiscetein	-7	-6.3
15.	Morin	-7.5	-6.5
16.	Fisetin	-7.7	-6.8
17.	Robinetin	-7.9	-6.7
18.	Luteolin	-7.4	-6.4
19.	Tricetin	-7.6	-6.6
20.	Apigenin	-7	-6.5
21.	Baicalein	-7.2	-6.5
22.	Remdesivir	-8.3	-7.7

To find out the possible reasons for the differences in the binding energies, we thoroughly analyzed the resulting complexes with the help of LigPlot⁺ software. **Table 2** and

Figure 1 show the potential interactions between remdesivir, GTP, EGCG, quercetagenin, and myricetin with SARS-CoV RdRp upon successful docking. GTP was involved in six hydrogen bond (H-bond) formation with RdRp residues Asp452, Arg553, Ala554, Thr556, Asp618 and Asp623, Additionally, GTP forms seven hydrophobic interactions with Arg555, Tyr455, Arg624, Cys622, Lys621, Tyr619 and Asp760 of SARS-CoV RdRp. Remdesivir forms six H-bonds with RdRp residues Arg553, Thr556, Cys622, Asp623, Arg624, Thr680 and twelve hydrophobic interactions with Val557, Tyr456, Tyr619, Asp760, Asp618, Lys798, Pro620, Lys621, Tyr455, Ser682, Ser681 and Ala558 as shown in **Figure 1a**. The large number of interactions accounts for the stability of the remdesivir-RdRp complex displaying the lowest binding energy of -8.3 kcal/mol.

EGCG which is the major polyphenol present in green tea and derived from leaves of the plant called as *Camellia sinensis*, upon docking established four H-bond interactions with Tyr456, Arg555, Thr556, Thr680 and nine hydrophobic interactions with Arg553, Asp452, Ala554, Tyr455, Arg624, Lys621, Asp623, Ser681, Ser682 of SARS-CoV RdRp. These interactions resulted in the lowest binding energy (-8.2 kcal/mol) for EGCG among all the twenty natural polyphenols studied. Wherein myricetin was involved in five H-bond interactions with Tyr456, Arg553, Arg624, Lys545, Thr680, and six hydrophobic interactions with Arg555, Asp623, Thr556, Ser681, Ser682, Met542 amino acid residue of SARS-CoV RdRp, this complex gave second-lowest binding energy of -8.1 kcal/mol. On the other hand, robinetin formed five hydrogen-bonds with Thr680, Thr556, Tyr456, Arg553, Arg624 and five hydrophobic interactions with Asp623, Met542, Arg555, Ser681, and Ser682 RdRp of SARS-CoV and these interactions resulting in -7.9 kcal/mol binding energy (**Figure S1a** in the Supplementary Information). Similarly, isorhamnetin formed six H-bond with Arg553, Arg555, Arg624, Lys545, Tyr456, Thr680 and seven hydrophobic interactions with RdRp residues Asp623, Thr556, Met542, Val557, Ala558 Ser681, Ser682 (**Figure S1b** in the Supplementary Information). Quercetagenin established six H-bond interactions with Arg553, Arg555 Arg624, Lys545, Tyr456, Thr680 and five hydrophobic interactions Asp623, Thr556, Met542, Ser681 and Ser682. Isorhamnetin and quercetagenin both formed six H-bond interactions with the same set of (Arg553, Arg555, Arg624, Lys545, Tyr456, Thr680) amino acid residues of SARS-CoV RdRp with same binding energy -7.8 kcal/mol. In summary, among the twenty selected polyphenols, five of them (EGCG, myricetin, robinetin, isorhamnetin, and quercetagenin) show a strong binding affinity towards SARS-CoV RdRp,

with binding energies comparable to GTP, a native nucleotide and an experimentally validated SARS-CoV-2 RdRp inhibitor, remdesivir.

Table 2: Ligand-amino acid interactions of top five scoring natural polyphenols against SARS-CoV RdRp

S. No.	Compound name	Binding energy (kcal/mol)	No. of non-covalent interactions	Involved amino acids
1	EGCG	-8.2	13	R555, R553, T556, D452, A554, Y455, R624, K621, Y456, D623, S681, T680, S682
2	Myricetin	-8.1	11	R553, R555, K545, D623, T556, T680, Y456, S681, S682, M542, R624
3	Robinetin	-7.9	10	D623, R624, M542, T556, Y456, R553, R555, T680, S681, S682
4	Quercetagetin	-7.8	11	R555, K545, T556, Y456, M542, S681, D623, S682, T680, D624, R553
5	Isorhamnetin	-7.8	13	R553, R555, K545, T556, D623, M542, Y456, A558, V557, T680, S681, S682, R624
6	Remdesivir (Control)	-8.3	18	V557, T680, Y456, D623, C622, Y619, D760, D618, K798, P620, K621, Y455, R553, R624, T556, S682, S681, A558
7	GTP (Control)	-8.2	13	R553, A554, R555, Y455, D452, R624, T556, D623, C622, K621, Y619, D618, D760

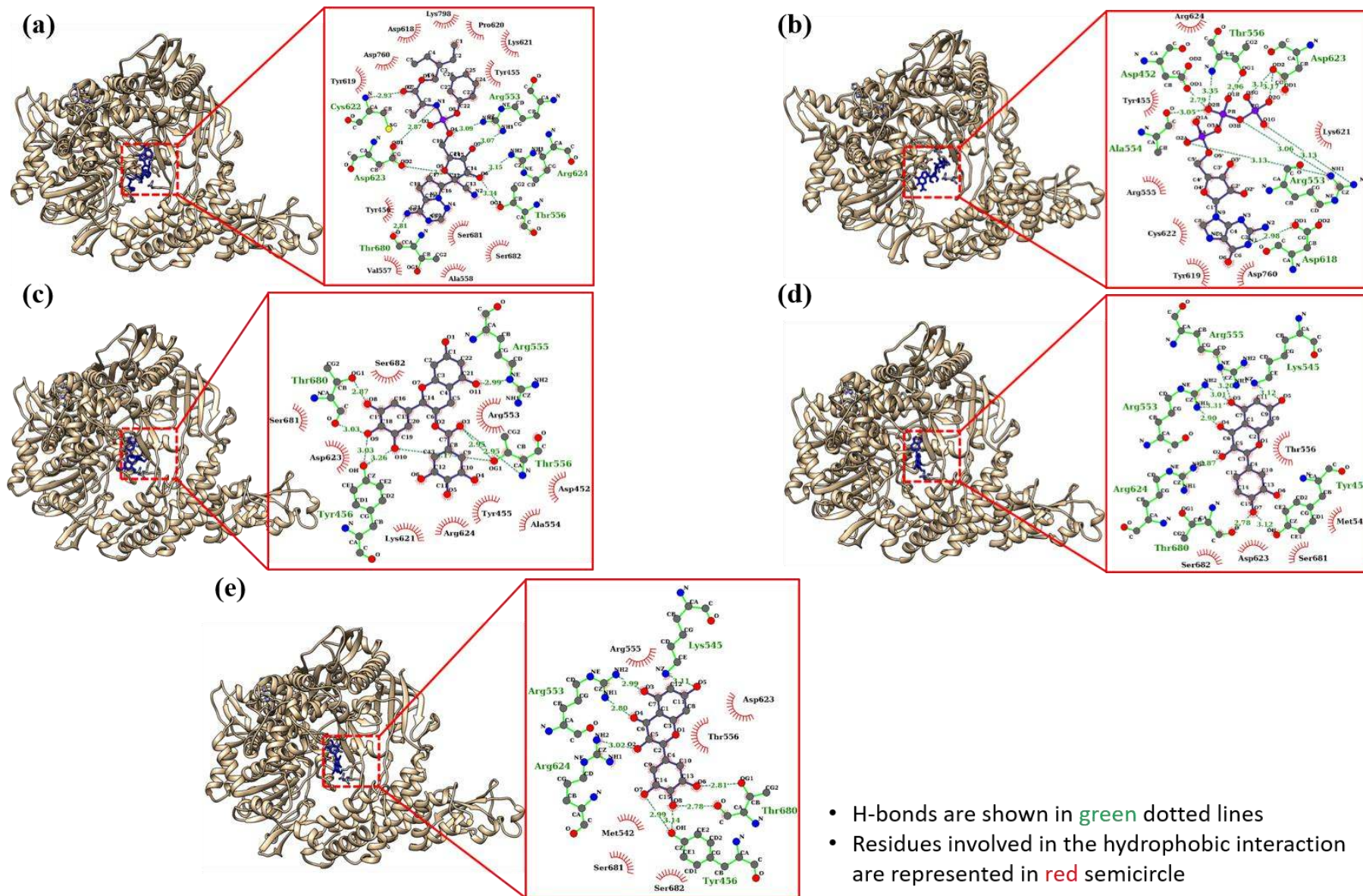


Figure 1. Best-docked conformation of SARS-CoV RdRp complexed with (a) remdesivir, (b) GTP, (c) EGCG, (d) quercetagenin, and (e) myricetin. Drug molecules are shown in stick model (blue). Amino acid residues interacting with the ligands are highlighted in the inset.

3.1.2 The binding mode analysis and predicted binding affinity calculations of natural polyphenols against the SARS-CoV-2 RdRp. Herein, we investigated our natural polyphenol library against RdRp of SARS-CoV-2 (PDB ID: 6M71) by molecular docking. Best conformation of the natural polyphenols was docked against SARS-CoV-2 RdRp and the resulting binding energies are shown in **Table 1**. The polyphenols exhibiting low binding energy (top five) against RdRp of SARS-CoV-2 are listed in **Table 3**. Control compounds, GTP and remdesivir again exhibited the lowest binding energy of -7.9 and -7.7 kcal/mol respectively against SARS-CoV-2 RdRp. Five polyphenols displayed significantly higher binding affinity among the selected twenty natural polyphenols docked against SARS-CoV-2 RdRp, with binding energies of EGCG, myricetin, quercetagenin, quercetin and curcumin as -7.3, -7.2, -6.9, -6.9, and -6.9 kcal/mol, respectively. Further 2D LigPlot representation of RdRp and the above-mentioned five natural polyphenols reveal the stable network of molecular interactions (**Figure 2, Table 3**).

For GTP-docked RdRp, the 2D LigPlot representation reveals ten H-bond with residues Arg624, Thr556, Asp623, Asp760, Tyr619, Cys622, Lys621, Asp452, Ala554, Arg553 and five hydrophobic interactions with Tyr455, Arg555, Asp761, Asp618, and Pro620. This large number of interactions account for the high stability of the complex with the lowest binding energy (-7.9 kcal/mol) among the series. Upon further analysis of the docking result, we observed that remdesivir forms five H-bonds with residues Arg553, Lys621, Cys622, Asp760, Glu811 and eight hydrophobic interactions with Trp800, Lys798, Pro620, Tyr455, Arg624, Tyr619, Asp618, Asp761. Similarly, LigPlot-generated files revealed that EGCG is forming four hydrogen bonds with Asp623, Tyr619, Lys621, Ser795 and five hydrophobic interactions with Cys622, Asp618, Met794, Pro620, Lys798. Moreover, myricetin binding environment by LigPlot analysis displayed five hydrogen bonds with Trp617, Trp800, Asp760, Glu811, Lys798 and five hydrophobic interactions with Asp618, Tyr619, Cys622, Asp761, Phe812. However, quercetagenin LigPlot analysis revealed five hydrogen bonds with Arg553, Arg555, Arg624, Thr556, Lys545 and three hydrophobic interactions with Lys621, Asp623, Tyr455. Whereas LigPlot analysis for quercetin established four H-bond interactions with Tyr619, Lys621, Asn691, Asp760 and four hydrophobic interactions Pro620, Cys622, Asp623, Arg553 (**Figure S2a** in the Supplementary Information). Curcumin formed two H-bond with Asp623, Ser795 and significantly high number (twelve) of hydrophobic interactions with Met794, Lys798, Asp618, Lys551, Lys621, Arg553, Tyr455, Arg624, Asp164, Phe793, Pro620, and Val166

(**Figure S2b** in the Supplementary Information). In addition to remdesivir, here we observed that three dietary polyphenols (EGCG, myricetin and quercetagenin) have significant potential to function as inhibitors of SARS-CoV-2 RdRp. Interestingly, the same three natural polyphenols (*i.e.* EGCG, myricetin and quercetagenin) appeared as the top-three scoring ligands for SARS-CoV RdRp (as highlighted in **Table 1**) as well suggesting that these set of natural polyphenols are expected to inhibit the RdRp activity and thus blocking the replication and preventing viral transcription. Many reports suggest polyphenols have low systemic toxicity and they are highly beneficial for human health (31). EGCG, a green tea polyphenol, has several pharmacological properties including antiviral activity (32,33). Similarly, myricetin has also been found to act as an inhibitor of the SARS coronavirus helicase (34). Quercetagenin also showed strong hepatitis C virus (HCV) replication inhibitory activity *in vitro* (15). Hence, these investigations indicate promising potential for the use of dietary polyphenols for the treatment of SARS-CoV-2 infection.

Table 3: Ligand-amino acid interactions of top five scoring natural polyphenols against SARS-CoV-2 RdRp

S. No.	Compound name	Binding energy (kcal/mol)	No. of non-covalent interactions	Involved amino acids
1	EGCG	-7.3	9	D623, Y619, K621, S795, C622, D618, M794, P620, K798
2	Myricetin	-7.2	10	W617, W800, D760, E811, K798, D618, Y619, C622, D761, F812
3	Quercetin	-6.9	8	Y619, K621, N691, D760, P620, C622, D623, R553
4	Quercetagenin	-6.9	8	R553, R555, R624, T556, K545, K621, D623, Y455
5	Curcumin	-6.9	14	D623, S795, M794, K798, D618, K551, K621, R553, Y455, R624, D164, F793, P620, V166
6	Remdesivir (Control)	-7.7	13	R553, K621, C622, D760, E811, W800, K798, P620, Y455, R624, Y619, D618, D761
7	GTP (Control)	-7.9	15	R624, T556, D623, D760, Y619, C622, K621, D452, A554, R553, Y455, R555, D761, D618, P620

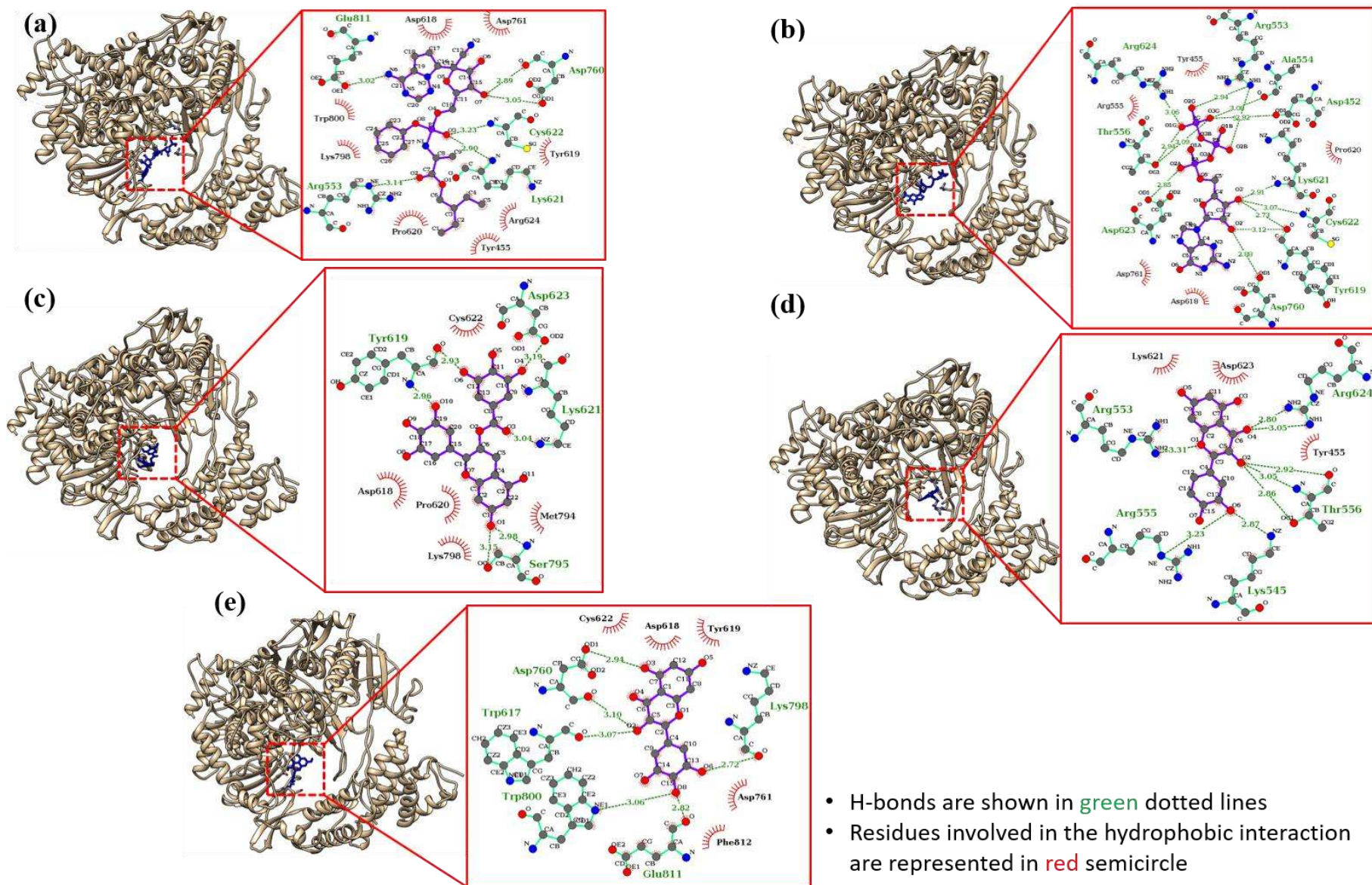


Figure 2. Best-docked conformation of SARS-CoV-2 RdRp complexed with (a) remdesivir, (b) GTP, (c) EGCG, (d) quercetagenin, and (e) myricetin. Drug molecules are shown in stick model (blue). Amino acid residues interacting with the ligands are highlighted in the inset.

3.2 Prediction of the absorption, distribution, metabolism, excretion, and toxicity (ADMET) profile

In addition to testing the physicochemical efficiency of a given molecule to inhibit the target protein, other parameters such as absorption, distribution, metabolism, excretion, and toxicity (ADMET) of the inhibitor play a critical role on demonstrating the likelihood of success of a drug. Utilization of *in-silico* ADMET profiling, in combination with *in vivo* and *in vitro* predictions in the initial stage of the screening process, can significantly fasten the drug discovery process by minimizing the number of potential safety problems. Hence, we performed a detailed ADMET profiling to evaluate the drug likeliness of the three polyphenols: EGCG, myricetin, quercetin that exhibited the highest score from the molecular docking study along with the positive control remdesivir.

Human colon adenocarcinoma-2 cell line (Caco2) permeability and human intestinal absorption (HIA) are key parameters to decide the total bioavailability of a drug. All the four compounds (EGCG, myricetin, quercetin and remdesivir) showed comparatively low Caco2 permeability potential ($<8 \times 10^{-6}$ cm/s) and could be absorbed *via* the human intestine (35). EGCG, myricetin, quercetin and remdesivir were predicted to be substrates of permeability glycoprotein (P-glycoprotein) which is an efflux membrane protein. However, remdesivir was predicted as a P-glycoprotein I inhibitor whereas EGCG as a P-glycoprotein II inhibitor. Hence, EGCG and remdesivir can regulate the physiological functions of P-glycoprotein (see **Table S2** in the Supplementary Information).

The distribution of a drug is regulated by many parameters such as lipid-solubility, concentration in plasma and binding ability to plasma proteins, transport proteins, etc. The volume of distribution at steady-state (VD_{ss}) suggests that remdesivir and EGCG had a lower theoretical dose required for uniform distribution in the plasma than myricetin and quercetin. Further, the degree of diffusion across the plasma membrane increases in the following order remdesivir < EGCG < myricetin < quercetin (**Table S3** in the Supplementary Information) as measured by the fraction that is in the unbound state. The predictions through the distribution of the drugs *via* the central nervous system and blood-brain barrier suggest that these four compounds are poorly distributed to the brain and unable to penetrate the central nervous system. However, the medium level of the lipophilicity of the drugs suggests that they would have no negative impact on nervous system exposure.

Cytochromes P450 (CYP) isozymes play crucial roles in drug metabolism. It has been observed that remdesivir is a substrate of CYP3A4 and hence, can be efficiently metabolized by CYP3A4. On the other hand, EGCG is CYP3A4 inhibitor, while myricetin and quercetagenin inhibit CYP1A2 (**Table S4** in the Supplementary Information). On a separate note, polyphenols are predominantly metabolized in the small intestine and liver by the conjugate formation of glucuronide, methyl sulfates in the urine and plasma (36).

Among the four compounds, none of them were predicted as the substrate of renal organic cation transporter-2 (Renal OCT2) as shown in **Table S5** in the Supplementary Information. This indicates that these compounds are possibly cleared through other available routes such as bile, breath, faces, and sweat. EGCG remains intact in the plasma and later excreted *via* bile and metabolized by colon microflora. It is also expected that all the compounds are absorbable *via* oral prescription.

We have also analyzed the toxicity profiles for EGCG, myricetin, quercetagenin as well as remdesivir (see **Table 4**). The toxicity prediction from the Ames test (*Salmonella typhimurium* reverse mutation assay) exhibited that all the compounds could be considered as non-mutagenic agents. High toxicity was observed for all the compounds in *Tetrahymena pyriformis*. Remdesivir and EGCG were shown to inhibit the human ether-a-go-go-related gene II (hERG II). However, Remdesivir has been shown to induce hepatotoxicity, whilst EGCG, myricetin, quercetagenin are not likely to be associated with hepatotoxicity. The maximum recommended tolerated dose (MRTD) in human prediction shows that remdesivir, myricetin, quercetagenin violate MRTD whereas natural polyphenol EGCG does not fall into this category. EGCG, myricetin, quercetagenin do not possess high acute toxicity whereas remdesivir regarded as high acute toxic compound as it falls under minnow toxicity. Additionally, none of the compounds predicted to be associated with skin sensitization.

Table 4: Predicted toxicity profile of EGCG, myricetin, quercetagenin and remdesivir

S. No.	Compounds name	Toxicity prediction	
		Properties	Predicted values
1	EGCG	AMES toxicity	No
		Maximum tolerated dose (Human)	0.441 (log mg/kg/day)
		hERG I inhibitor	No
		hERG II inhibitor	Yes
		Oral rat acute toxicity (LD ₅₀)	2.522 (mol/kg)
		Oral rat chronic toxicity (LOAEL)	3.065 (log mg/kg_bw/day)
		Hepatotoxicity	No

		Skin sensitivity	No
		<i>T. pyriformis</i> toxicity	0.285 (µg/L)
		Minnow toxicity	7.713 log mM
2	Myricetin	AMES toxicity	No
		Maximum tolerated dose (Human)	0.51 (log mg/kg/day)
		hERG I inhibitor	No
		hERG II inhibitor	No
		Oral rat acute toxicity (LD ₅₀)	2.497 (mol/kg)
		Oral rat chronic toxicity (LOAEL)	2.718 (log mg/kg_bw/day)
		Hepatotoxicity	No
		Skin sensitivity	No
		<i>T. pyriformis</i> toxicity	0.286 (µg/L)
		Minnow toxicity	5.023 log mM
3	Quercetagenin	AMES toxicity	No
		Maximum tolerated dose (Human)	0.486 (log mg/kg/day)
		hERG I inhibitor	No
		hERG II inhibitor	No
		Oral rat acute toxicity (LD ₅₀)	2.537 (mol/kg)
		Oral rat chronic toxicity (LOAEL)	3.185 (log mg/kg_bw/day)
		Hepatotoxicity	No
		Skin sensitivity	No
		<i>T. pyriformis</i> toxicity	0.285 (µg/L)
		Minnow toxicity	3.475 log mM
4	Remdesivir	AMES toxicity	No
		Maximum tolerated dose (Human)	0.15 (log mg/kg/day)
		hERG I inhibitor	No
		hERG II inhibitor	Yes
		Oral rat acute toxicity (LD ₅₀)	2.043 (mol/kg)
		Oral rat chronic toxicity (LOAEL)	1.639 (log mg/kg_bw/day)
		Hepatotoxicity	Yes
		Skin sensitivity	No
		<i>T. pyriformis</i> toxicity	0.285 (µg/L)
		Minnow toxicity	0.291 log mM

3.3 Identification of target class for natural polyphenol *via* target prediction studies

The polyphenolic structural motif of dietary polyphenols allows them to serve as excellent hydrogen bond donors which in turn helps them to strongly interact with various biomacromolecules such as proteins. This interaction is a critical step in the regulatory role of polyphenols on various key proteins involved in cellular physiology. The majority, if not all, of the beneficial effect of polyphenols, can be explained via the functional consequence of proteins it interacts with. Molecular target studies help us to predict therapeutic protein targets for a given small molecule. Herein, we analyzed the predicted interacting proteins/enzymes for myricetin, quercetagenin and EGCG. This study is particularly

important in that context as we believe these polyphenols could target RdRp, an important enzyme that catalyzes the RNA replication in SARS-COV-2. Notably, the molecular target analysis suggests that all three polyphenols possess excellent properties of druggability and they interact with a diverse class of proteins/enzymes. The top 25 target classes of EGCG, myricetin, quercetagetin and remdesivir are represented in the pie-chart as shown in **Figure 3**. The detailed output table with the target, common name, UniProt ID, ChEMBL ID, target class, probability and known actives in 2D/3D are listed in **Figure S3-6** in the Supplementary Information.

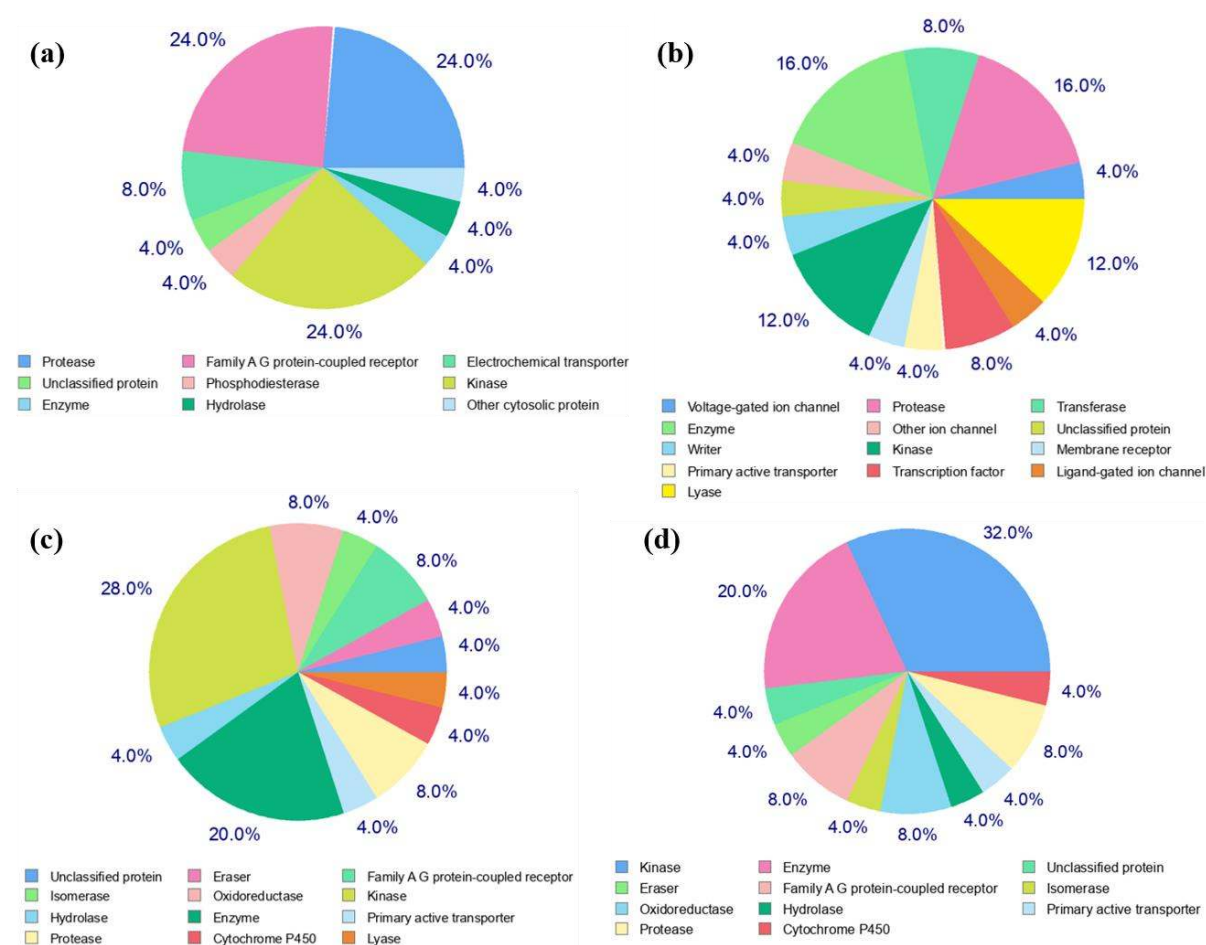


Figure 3. Molecular target predictions for (a) remdesivir, (b) EGCG, (c) myricetin, (d) quercetagetin obtained from swiss target prediction report. The frequency of the target classes (top 25) is depicted in the pie chart.

4. Conclusions

At present, COVID-19 caused by the SARS-CoV-2 infection is a massive threat to global health. During the SARS outbreak caused by SARS-CoV in 2003 ended up infecting 8094 and killing 774 people with a mortality rate of ~9.5%. Although the mortality rate in SARS-

CoV-2 infection is lower than other similar viral infections, the extremely high number of infections and death in a rather short period of time has triggered this alarming situation. More importantly, there exists no specific vaccine or antiviral drug that can tackle this COVID-19 pandemic. However, many clinical trials are being carried out for drugs as well as vaccines against SARS-CoV-2. In this work, we performed a comprehensive molecular docking study with twenty natural polyphenols with potential antiviral properties that may inhibit the SARS-CoV-2 RdRp and prevent the RNA replication. We also looked at the ADME prediction, toxicity prediction and target analysis to assess their druggability. The obtained results strongly suggest that (-)-epigallocatechin-3-gallate (EGCG), myricetin and quercetagenin have high binding affinity towards the RdRp of both SARS-CoV and SARS-CoV-2 with favorable pharmacokinetics properties. As these polyphenolic compounds are of natural origin and being consumed since ancient times, they do not possess any inherent cytotoxicity. These bioactive compounds exhibit broad ranges of therapeutic properties. Therefore, we believe that these three natural polyphenols can act as potential inhibitors for RdRp of SARS-CoV-2. However, further *in vitro* and *in vivo* studies are recommended to validate their efficacy against SARS-CoV-2 infection.

Acknowledgments. The authors gratefully acknowledge the financial support from the Indian Institute of Technology Indore and Indian Institute of Technology Palakkad for the provision of conducting research and the scholarship provided by the Ministry of Human Resource Development, Govt. of India to S. Singh. This work was also supported by the Department of Science and Technology-Science & Engineering Research Board (DST-SERB), Govt. of India (ECR/2017/002082).

Conflicts of interest. The authors declare that there is no conflict of interest.

5. References

1. Chan, J. F., Lau, S. K., To, K. K., Cheng, V. C., Woo, P. C., and Yuen, K.-Y. (2015) Middle East respiratory syndrome coronavirus: another zoonotic betacoronavirus causing SARS-like disease. *Clin Microbiol Rev.* **28**, 465-522
2. Ibrahim, I. M., Abdelmalek, D. H., Elshahat, M. E., and Elfiky, A. A. (2020) COVID-19 spike-host cell receptor GRP78 binding site prediction. *J Infect.*
3. Wu, F., Zhao, S., Yu, B., Chen, Y.-M., Wang, W., Song, Z.-G., Hu, Y., Tao, Z.-W., Tian, J.-H., and Pei, Y.-Y. (2020) A new coronavirus associated with human respiratory disease in China. *Nature* **579**, 265-269

4. Zhai, Y., Sun, F., Li, X., Pang, H., Xu, X., Bartlam, M., and Rao, Z. (2005) Insights into SARS-CoV transcription and replication from the structure of the nsp7–nsp8 hexadecamer. *Nat Struct Mol Biol.* **12**, 980-986
5. Subissi, L., Posthuma, C. C., Collet, A., Zevenhoven-Dobbe, J. C., Gorbalenya, A. E., Decroly, E., Snijder, E. J., Canard, B., and Imbert, I. (2014) One severe acute respiratory syndrome coronavirus protein complex integrates processive RNA polymerase and exonuclease activities. *Proc Natl Acad Sci USA.* **111**, E3900-E3909
6. Yin, W., Mao, C., Luan, X., Shen, D.-D., Shen, Q., Su, H., Wang, X., Zhou, F., Zhao, W., and Gao, M. (2020) Structural basis for inhibition of the RNA-dependent RNA polymerase from SARS-CoV-2 by remdesivir. *Science*
7. Elfiky, A. A. (2017) Zika virus: novel guanosine derivatives revealed strong binding and possible inhibition of the polymerase. *Future Virol.* **12**, 721-728
8. Elfiky, A. A. (2019) Novel guanosine derivatives as anti-HCV NS5b polymerase: a QSAR and molecular docking study. *Med Chem.* **15**, 130-137
9. Ganesan, A., and Barakat, K. (2017) Applications of computer-aided approaches in the development of hepatitis C antiviral agents. *Expert Opin Drug Discov.* **12**, 407-425
10. Elfiky, A. A. (2020) Anti-HCV, nucleotide inhibitors, repurposing against COVID-19. *Life Sci.*, 117477
11. Jia, H., and Gong, P. (2019) A structure-function diversity survey of the RNA-dependent RNA polymerases from the positive-strand RNA viruses. *Front Microbiol.* **10**, 1945
12. Wu, J., and Gong, P. (2018) Visualizing the nucleotide addition cycle of viral RNA-dependent RNA polymerase. *Viruses* **10**, 24
13. Szajdek, A., and Borowska, E. (2008) Bioactive compounds and health-promoting properties of berry fruits: a review. *Plant Foods Hum Nutr.* **63**, 147-156
14. Lin, L.-T., Hsu, W.-C., and Lin, C.-C. (2014) Antiviral natural products and herbal medicines. *J Tradit Complement Med.* **4**, 24-35
15. Ahmed-Belkacem, A., Guichou, J.-F., Brillet, R., Ahnou, N., Hernandez, E., Pallier, C., and Pawlotsky, J.-M. (2014) Inhibition of RNA binding to hepatitis C virus RNA-dependent RNA polymerase: a new mechanism for antiviral intervention. *Nucleic Acids Res.* **42**, 9399-9409
16. Song, J.-M., Lee, K.-H., and Seong, B.-L. (2005) Antiviral effect of catechins in green tea on influenza virus. *Antiviral Res.* **68**, 66-74
17. Kuzuhara, T., Iwai, Y., Takahashi, H., Hatakeyama, D., and Echigo, N. (2009) Green tea catechins inhibit the endonuclease activity of influenza A virus RNA polymerase. *PLoS Curr.* **1**
18. Ho, H.-Y., Cheng, M.-L., Weng, S.-F., Leu, Y.-L., and Chiu, D. T.-Y. (2009) Antiviral effect of epigallocatechin gallate on enterovirus 71. *J Agric Food Chem.* **57**, 6140-6147
19. Kirchdoerfer, R. N., and Ward, A. B. (2019) Structure of the SARS-CoV nsp12 polymerase bound to nsp7 and nsp8 co-factors. *Nat Commun.* **10**, 1-9
20. Yan, R., Zhang, Y., Li, Y., Xia, L., Guo, Y., and Zhou, Q. (2020) Structural basis for the recognition of SARS-CoV-2 by full-length human ACE2. *Science* **367**, 1444-1448
21. Berman, H. M., Bhat, T. N., Bourne, P. E., Feng, Z., Gilliland, G., Weissig, H., and Westbrook, J. (2000) The Protein Data Bank and the challenge of structural genomics. *Nat Struct Biol.* **7**, 957-959
22. Morris, G. M., Huey, R., Lindstrom, W., Sanner, M. F., Belew, R. K.,Goodsell, D. S., and Olson, A. J. (2009) AutoDock4 and AutoDockTools4: Automated docking with selective receptor flexibility. *J Comput Chem.* **30**, 2785-2791

23. Kim, S., Chen, J., Cheng, T., Gindulyte, A., He, J., He, S., Li, Q., Shoemaker, B. A., Thiessen, P. A., and Yu, B. (2019) PubChem 2019 update: improved access to chemical data. *Nucleic Acids Res.* **47**, D1102-D1109
24. Pettersen, E. F., Goddard, T. D., Huang, C. C., Couch, G. S., Greenblatt, D. M., Meng, E. C., and Ferrin, T. E. (2004) UCSF Chimera—a visualization system for exploratory research and analysis. *J Comput Chem.* **25**, 1605-1612
25. Trott, O., and Olson, A. J. (2010) AutoDock Vina: improving the speed and accuracy of docking with a new scoring function, efficient optimization, and multithreading. *J Comput Chem.* **31**, 455-461
26. Wallace, A. C., Laskowski, R. A., and Thornton, J. M. (1995) LIGPLOT: a program to generate schematic diagrams of protein-ligand interactions. *Protein Eng Des Sel.* **8**, 127-134
27. Pires, D. E., Blundell, T. L., and Ascher, D. B. (2015) pkCSM: predicting small-molecule pharmacokinetic and toxicity properties using graph-based signatures. *J Med Chem.* **58**, 4066-4072
28. Gfeller, D., Grosdidier, A., Wirth, M., Daina, A., Michielin, O., and Zoete, V. (2014) SwissTargetPrediction: a web server for target prediction of bioactive small molecules. *Nucleic Acids Res.* **42**, W32-W38
29. Agostini, M. L., Andres, E. L., Sims, A. C., Graham, R. L., Sheahan, T. P., Lu, X., Smith, E. C., Case, J. B., Feng, J. Y., and Jordan, R. (2018) Coronavirus susceptibility to the antiviral remdesivir (GS-5734) is mediated by the viral polymerase and the proofreading exoribonuclease. *mBio* **9**, e00221-00218
30. Gordon, C. J., Tchesnokov, E. P., Woolner, E., Perry, J. K., Feng, J. Y., Porter, D. P., and Gotte, M. (2020) Remdesivir is a direct-acting antiviral that inhibits RNA-dependent RNA polymerase from severe acute respiratory syndrome coronavirus 2 with high potency. *J Biol Chem.*, jbc.RA120.013679
31. Cory, H., Passarelli, S., Szeto, J., Tamez, M., and Mattei, J. (2018) The role of polyphenols in human health and food systems: a mini-review. *Front Nutr.* **5**, 87
32. Moon, Y. J., and Morris, M. E. (2007) Pharmacokinetics and bioavailability of the bioflavonoid biochanin A: effects of quercetin and EGCG on biochanin A disposition in rats. *Mol Pharm.* **4**, 865-872
33. Carneiro, B. M., Batista, M. N., Braga, A. C. S., Nogueira, M. L., and Rahal, P. (2016) The green tea molecule EGCG inhibits Zika virus entry. *Virology* **496**, 215-218
34. Yu, M.-S., Lee, J., Lee, J. M., Kim, Y., Chin, Y.-W., Jee, J.-G., Keum, Y.-S., and Jeong, Y.-J. (2012) Identification of myricetin and scutellarein as novel chemical inhibitors of the SARS coronavirus helicase, nsP13. *Bioorg Med Chem Lett.* **22**, 4049-4054
35. Larregieu, C. A., and Benet, L. Z. (2013) Drug discovery and regulatory considerations for improving in silico and in vitro predictions that use Caco-2 as a surrogate for human intestinal permeability measurements. *AAPS J.* **15**, 483-497
36. Chow, H. S., Hakim, I. A., Vining, D. R., Crowell, J. A., Ranger-Moore, J., Chew, W. M., Celaya, C. A., Rodney, S. R., Hara, Y., and Alberts, D. S. (2005) Effects of dosing condition on the oral bioavailability of green tea catechins after single-dose administration of Polyphenon E in healthy individuals. *Clin Cancer Res.* **11**, 4627-4633

Supplementary Information

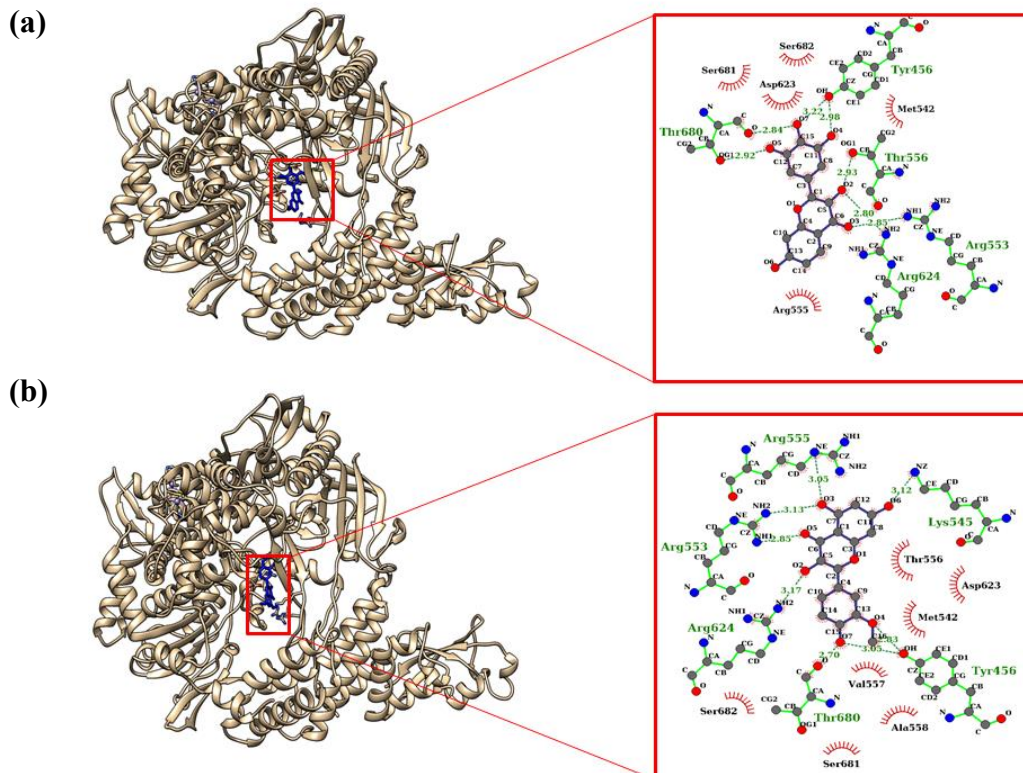


Figure S1. Best-docked conformation of SARS-CoV RdRp complexed with (a) robinetin, (b) isorhamnetin drug molecules are shown in stick model (blue). Amino acid residues interacting with the ligands are highlighted in the inset.

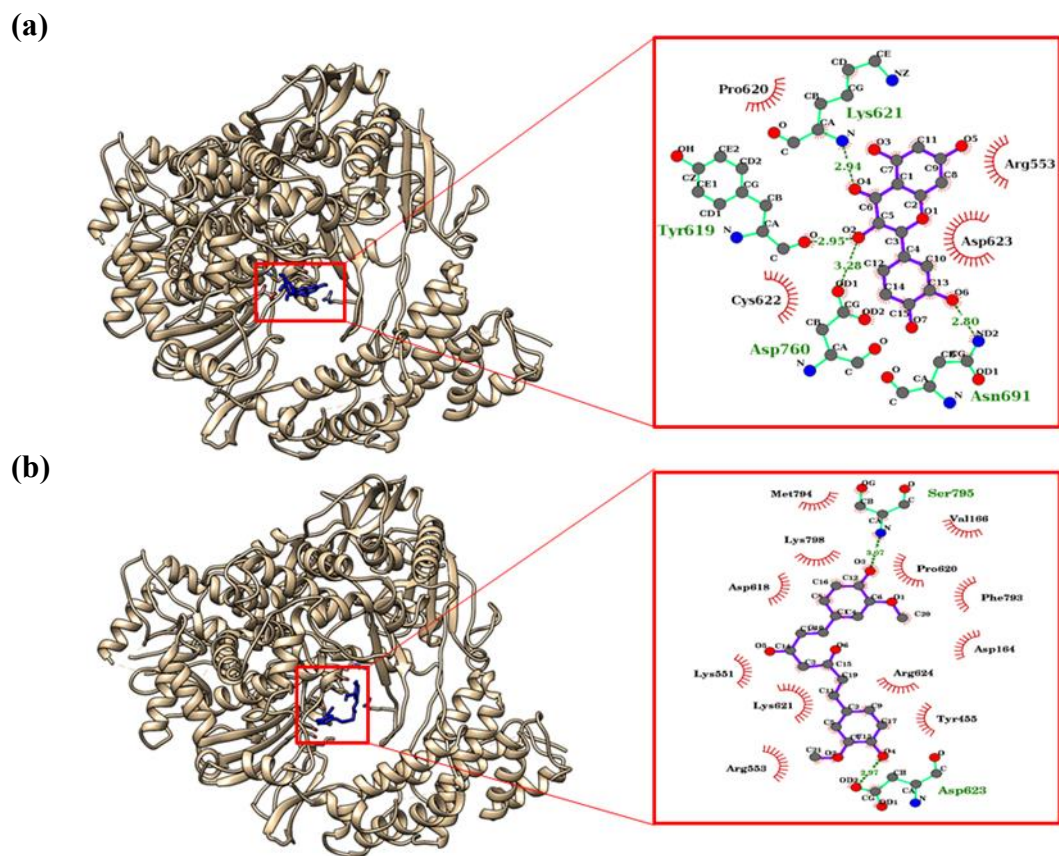


Figure S2. Best docked conformation of SARS-CoV-2 RdRp complexed with (a) quercetin, (b) curcumin. Drug molecules are shown in stick model (blue). Amino acid residues interacting with the ligands are highlighted in the inset.

Target	Common name	Uniprot ID	ChEMBL ID	Target Class	Probability*	Known actives (3D/2D)
Matrix metalloproteinase 13	MMP13	P45452	CHEMBL280	Protease		235 / 0 ↓
Adenosine A2a receptor	ADORA2A	P29274	CHEMBL251	Family A G protein-coupled receptor		529 / 0 ↓
Adenosine A3 receptor	ADORA3	P0DMS8	CHEMBL256	Family A G protein-coupled receptor		610 / 0 ↓
Adenosine A1 receptor	ADORA1	P30542	CHEMBL226	Family A G protein-coupled receptor		697 / 0 ↓
Sodium/glucose cotransporter 2	SLC5A2	P31639	CHEMBL3884	Electrochemical transporter		254 / 0 ↓
Transmembrane domain-containing protein TMIGD3	TMIGD3	P0DMS9	CHEMBL3712907	Unclassified protein		33 / 0 ↓
Sodium/glucose cotransporter 1	SLC5A1	P13866	CHEMBL4979	Electrochemical transporter		46 / 0 ↓
Phosphodiesterase 5A	PDE5A	O76074	CHEMBL1827	Phosphodiesterase		119 / 0 ↓
ADAM17	ADAM17	P78536	CHEMBL3706	Protease		169 / 0 ↓
Serine/threonine-protein kinase Aurora-B	AURKB	Q96GD4	CHEMBL2185	Kinase		113 / 0 ↓
Serine/threonine-protein kinase Aurora-A	AURKA	O14965	CHEMBL4722	Kinase		168 / 0 ↓
Adenosine A2b receptor	ADORA2B	P29275	CHEMBL255	Family A G protein-coupled receptor		54 / 0 ↓
MAP kinase ERK2	MAPK1	P28482	CHEMBL4040	Kinase		212 / 0 ↓
Coagulation factor IX	F9	P00740	CHEMBL2016	Protease		16 / 0 ↓
Matrix metalloproteinase 9	MMP9	P14780	CHEMBL321	Protease		137 / 0 ↓
Matrix metalloproteinase 2	MMP2	P08253	CHEMBL333	Protease		158 / 0 ↓
Endothelin receptor ET-B	EDNRB	P24530	CHEMBL1785	Family A G protein-coupled receptor		93 / 0 ↓
Endothelin receptor ET-A	EDNRA	P25101	CHEMBL252	Family A G protein-coupled receptor		127 / 0 ↓
Hexokinase type IV	GCK	P35557	CHEMBL3820	Enzyme		83 / 0 ↓
Endothelial lipase	LIPG	Q9Y5X9	CHEMBL5080	Hydrolase		43 / 0 ↓
Tyrosine-protein kinase receptor FLT3	FLT3	P36888	CHEMBL1974	Kinase		35 / 0 ↓
Beta-secretase 1	BACE1	P56817	CHEMBL4822	Protease		525 / 0 ↓
Protein kinase C alpha	PRKCA	P17252	CHEMBL299	Kinase		94 / 0 ↓
RAS guanyl releasing protein 3	RASGRP3	Q8IV61	CHEMBL3638	Other cytosolic protein		38 / 0 ↓
Cyclin-dependent kinase 5/CDK5 activator 1	CDK5R1 CDK5	Q15078 Q00535	CHEMBL1907600	Kinase		43 / 0 ↓

Figure S3. SwissTargetPrediction report obtained using remdesivir as the query molecule.

Target	Common name	Uniprot ID	ChEMBL ID	Target Class	Probability*	Known actives (3D/2D)
HERG	KCNH2	Q12809	CHEMBL240	Voltage-gated ion channel		2 / 1
Beta-secretase 1	BACE1	P56817	CHEMBL4822	Protease		40 / 14
CMP-N-acetylneuraminate-beta-1,4-galactoside alpha-2,3-sialyltransferase	ST3GAL3	Q11203	CHEMBL3596076	Transferase		1 / 1
Alpha-(1,3)-fucosyltransferase 7	FUT7	Q11130	CHEMBL3596077	Transferase		1 / 1
Fucosyltransferase 4	FUT4	P22083	CHEMBL4996	Enzyme		1 / 1
Apoptosis regulator Bcl-2	BCL2	P10415	CHEMBL4860	Other ion channel		5 / 7
Matrix metalloproteinase 2	MMP2	P08253	CHEMBL333	Protease		28 / 6
Matrix metalloproteinase 14	MMP14	P50281	CHEMBL3869	Protease		10 / 4
Microtubule-associated protein tau	MAPT	P10636	CHEMBL1293224	Unclassified protein		2 / 1
DNA (cytosine-5)-methyltransferase 1	DNMT1	P26358	CHEMBL1993	Writer		1 / 1
Dual-specificity tyrosine-phosphorylation regulated kinase 1A	DYRK1A	Q13627	CHEMBL2292	Kinase		12 / 1
Beta amyloid A4 protein	APP	P05067	CHEMBL2487	Membrane receptor		13 / 2
MAP kinase p38 alpha	MAPK14	Q16539	CHEMBL260	Kinase		2 / 2
Telomerase reverse transcriptase	TERT	O14746	CHEMBL2916	Enzyme		6 / 2
6-phosphogluconate dehydrogenase	PGD	P52209	CHEMBL3404	Enzyme		4 / 4
Hepatocyte growth factor receptor	MET	P08581	CHEMBL3717	Kinase		17 / 6
P-glycoprotein 1	ABCB1	P08183	CHEMBL4302	Primary active transporter		3 / 99
Signal transducer and activator of transcription 1-alpha/beta	STAT1	P42224	CHEMBL6101	Transcription factor		1 / 1
Squalene monooxygenase (<i>by homology</i>)	SQLE	Q14534	CHEMBL3592	Enzyme		1 / 9
GABA-A receptor, alpha-1/beta-2/gamma-2	GABRA1 GABRB2 GABRG2	P14867 P47870 P18507	CHEMBL2095172	Ligand-gated ion channel		0 / 1
Carbonic anhydrase III	CA3	P07451	CHEMBL2885	Lyase		0 / 2
Matrix metalloproteinase 12	MMP12	P39900	CHEMBL4393	Protease		4 / 6
Hypoxia-inducible factor 1 alpha	HIF1A	Q16665	CHEMBL4261	Transcription factor		0 / 6
Carbonic anhydrase II	CA2	P00918	CHEMBL205	Lyase		26 / 2
Carbonic anhydrase I	CA1	P00915	CHEMBL261	Lyase		27 / 2

Figure S4. SwissTargetPrediction report obtained using EGCG as the query molecule.

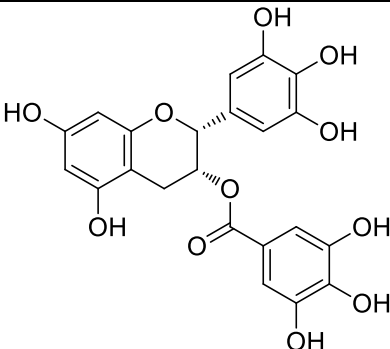
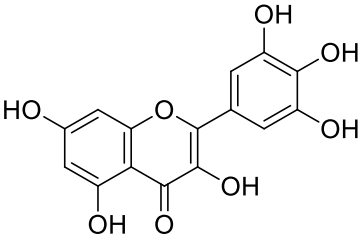
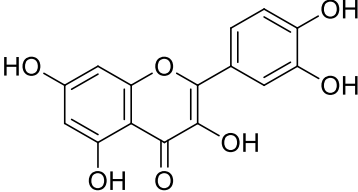
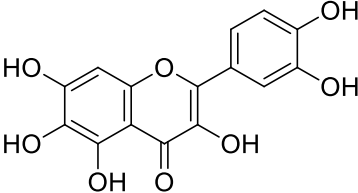
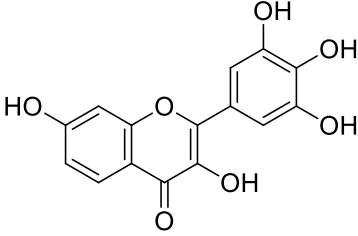
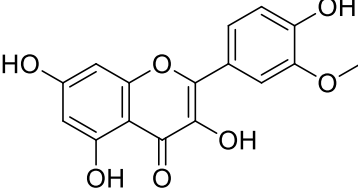
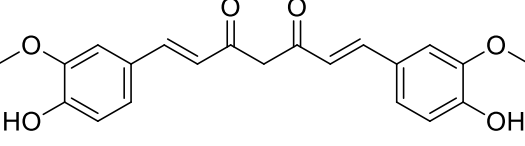
Target	Common name	Uniprot ID	ChEMBL ID	Target Class	Probability*	Known actives (3D/2D)
Microtubule-associated protein tau	MAPT	P10636	CHEMBL1293224	Unclassified protein		1 / 1
Lysine-specific demethylase 4D-like	KDM4E	B2RXH2	CHEMBL1293226	Eraser		1 / 2
G-protein coupled receptor 35	GPR35	Q9HC97	CHEMBL1293267	Family A G protein-coupled receptor		2 / 4
DNA topoisomerase II alpha	TOP2A	P11388	CHEMBL1806	Isomerase		1 / 1
Xanthine dehydrogenase	XDH	P47989	CHEMBL1929	Oxidoreductase		10 / 20
Tyrosine-protein kinase receptor FLT3	FLT3	P36888	CHEMBL1974	Kinase		5 / 7
Insulin receptor	INSR	P06213	CHEMBL1981	Kinase		1 / 1
Acetylcholinesterase	ACHE	P22303	CHEMBL220	Hydrolase		3 / 27
Glyoxalase I	GLO1	Q04760	CHEMBL2424	Enzyme		3 / 4
Myosin light chain kinase, smooth muscle	MYLK	Q15746	CHEMBL2428	Kinase		1 / 1
Tyrosine-protein kinase SYK	SYK	P43405	CHEMBL2599	Kinase		3 / 3
Multidrug resistance-associated protein 1	ABCC1	P33527	CHEMBL3004	Primary active transporter		7 / 11
PI3-kinase p110-gamma subunit	PIK3CG	P48736	CHEMBL3267	Enzyme		1 / 1
Beta-secretase 1	BACE1	P56817	CHEMBL4822	Protease		8 / 14
DNA-(apurinic or apyrimidinic site) lyase	APEX1	P27695	CHEMBL5619	Enzyme		1 / 1
NADPH oxidase 4	NOX4	Q9NPH5	CHEMBL1250375	Enzyme		6 / 8
Vasopressin V2 receptor	AVPR2	P30518	CHEMBL1790	Family A G protein-coupled receptor		1 / 1
Aldose reductase	AKR1B1	P15121	CHEMBL1900	Enzyme		18 / 72
Monoamine oxidase A	MAOA	P21397	CHEMBL1951	Oxidoreductase		4 / 14
Insulin-like growth factor I receptor	IGF1R	P08069	CHEMBL1957	Kinase		3 / 3
Cytochrome P450 19A1	CYP19A1	P11511	CHEMBL1978	Cytochrome P450		3 / 18
Epidermal growth factor receptor erbB1	EGFR	P00533	CHEMBL203	Kinase		4 / 28
Thrombin	F2	P00734	CHEMBL204	Protease		11 / 3
Carbonic anhydrase II	CA2	P00918	CHEMBL205	Lyase		4 / 15
Serine/threonine-protein kinase PIM1	PIM1	P11309	CHEMBL2147	Kinase		6 / 7

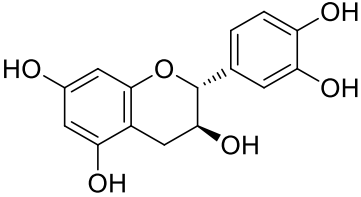
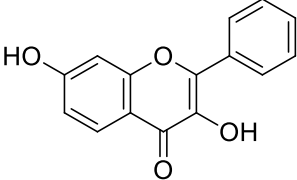
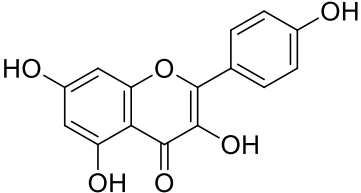
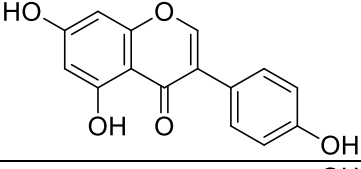
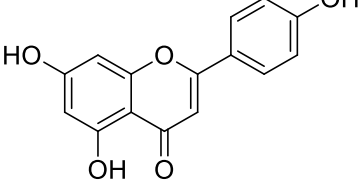
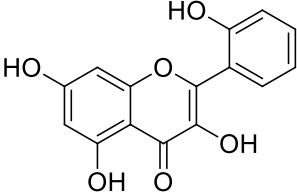
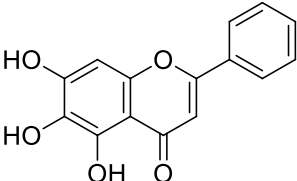
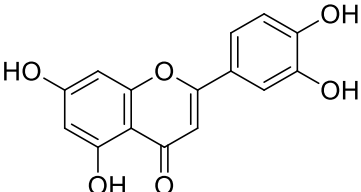
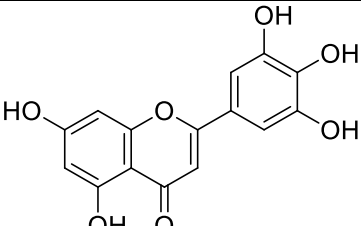
Figure S5. SwissTargetPrediction report obtained using myricetin as the query molecule.

Target	Common name	Uniprot ID	ChEMBL ID	Target Class	Probability*	Known actives (3D/2D)
Serine/threonine-protein kinase PIM1	PIM1	P11309	CHEMBL2147	Kinase		7 / 7
Aldose reductase	AKR1B1	P15121	CHEMBL1900	Enzyme		21 / 72
Microtubule-associated protein tau	MAPT	P10636	CHEMBL1293224	Unclassified protein		1 / 1
Lysine-specific demethylase 4D-like	KDM4E	B2RXH2	CHEMBL1293226	Eraser		2 / 2
G-protein coupled receptor 35	GPR35	Q9HC97	CHEMBL1293267	Family A G protein-coupled receptor		2 / 4
DNA topoisomerase II alpha	TOP2A	P11388	CHEMBL1806	Isomerase		1 / 1
Xanthine dehydrogenase	XDH	P47989	CHEMBL1929	Oxidoreductase		11 / 20
Tyrosine-protein kinase receptor FLT3	FLT3	P36888	CHEMBL1974	Kinase		5 / 7
Insulin receptor	INSR	P06213	CHEMBL1981	Kinase		1 / 1
Acetylcholinesterase	ACHE	P22303	CHEMBL220	Hydrolase		3 / 27
Glyoxalase I	GLO1	Q04760	CHEMBL2424	Enzyme		3 / 4
Myosin light chain kinase, smooth muscle	MYLK	Q15746	CHEMBL2428	Kinase		1 / 1
Tyrosine-protein kinase SYK	SYK	P43405	CHEMBL2599	Kinase		3 / 3
Multidrug resistance-associated protein 1	ABCC1	P33527	CHEMBL3004	Primary active transporter		7 / 11
PI3-kinase p110-gamma subunit	PIK3CG	P48736	CHEMBL3267	Enzyme		3 / 1
Beta-secretase 1	BACE1	P56817	CHEMBL4822	Protease		6 / 14
DNA-(apurinic or apyrimidinic site) lyase	APEX1	P27695	CHEMBL5619	Enzyme		1 / 1
Death-associated protein kinase 1	DAPK1	P53355	CHEMBL2558	Kinase		2 / 2
NADPH oxidase 4	NOX4	Q9NPH5	CHEMBL1250375	Enzyme		6 / 8
Vasopressin V2 receptor	AVPR2	P30518	CHEMBL1790	Family A G protein-coupled receptor		1 / 1
Monoamine oxidase A	MAOA	P21397	CHEMBL1951	Oxidoreductase		4 / 15
Insulin-like growth factor I receptor	IGF1R	P08069	CHEMBL1957	Kinase		4 / 3
Cytochrome P450 19A1	CYP19A1	P11511	CHEMBL1978	Cytochrome P450		2 / 17
Epidermal growth factor receptor erbB1	EGFR	P00533	CHEMBL203	Kinase		4 / 28
Thrombin	F2	P00734	CHEMBL204	Protease		6 / 3

Figure S6. SwissTargetPrediction report obtained using quercetagenin as the query molecule.

Table S1. Chemical structure and natural source for the twenty polyphenols selected for the current study.

S. No.	Compound (PubChem CID No.)	Structure	Common Sources
1	EGCG (65064)		<i>Camellia sinensis</i>
2	Myricetin (5281672)		<i>Solanum lycopersicum</i>
3	Quercetin (5280343)		<i>Alium cepa</i>
4	Quercetagetin (5281680)		<i>Citrus limon</i>
5	Robinetin (5280647)		<i>Vaccinium corymbosum</i>
6	Isorhamnetin (5281654)		<i>Solanum lycopersicum</i>
7	Curcumin (969516)		<i>Curcuma longa</i>

8	Catechin (73160)		<i>Vitis vinifera</i>
9	5-Deoxygalangin (5393152)		<i>Spatholobus subrectus</i>
10	Kaempferol (5280863)		<i>Brassica oleracea var. italica</i>
11	Genistein (5280961)		<i>Coffea arabica</i>
12	Apigenin (5280443)		<i>Camellia sinensis</i>
13	Datisctin (5281610)		<i>Datisca cannabina</i>
14	Baicalein (5281605)		<i>Oroxylum indicum</i>
15	Luteolin (5280445)		<i>Piper nigrum</i>
16	Tricetin (5281701)		<i>Eucalyptus globus</i>

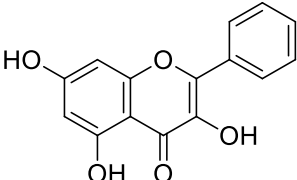
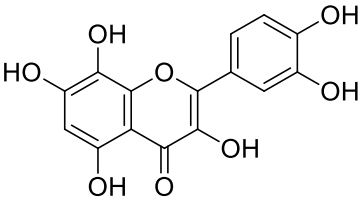
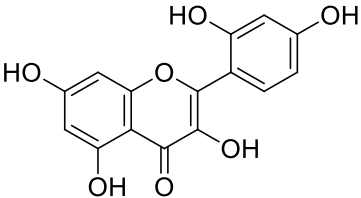
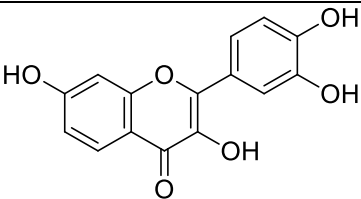
17	Galangin (5281616)		<i>Alpinia officinarum</i>
18	Gossypetin (5280647)		<i>Hibiscus sabdariffa</i>
19	Morin (5281670)		<i>Psidium guajava</i>
20	Fisetin (5281614)		<i>Malus domestica</i>

Table S2: Predicted absorption properties of remdesivir, EGCG, myricetin and quercetagenin

Properties	Remdesivir	EGCG	Myricetin	Quercetagenin
Water solubility log mol/L	-3.07	-2.894	-2.915	-2.904
Caco2 permeability Log 10 ⁻⁶ cm/s	0.635	-1.521	0.095	-1.488
Human intestinal absorption (%)	71.109	47.395	65.93	62.773
Skin permeability log Kp	-2.735	-2.735	-2.735	-2.735
P-glycoprotein substrate	Yes	Yes	Yes	Yes
P-glycoprotein I inhibitor	Yes	No	No	No
P-glycoprotein II inhibitor	No	Yes	No	No

Table S3: Predicted distribution properties of remdesivir, EGCG, myricetin and quercetagenin

Properties	Remdesivir	EGCG	Myricetin	Quercetagenin
VD _{ss} (log L/kg)	0.307	0.806	1.317	1.424
Fraction unbound (human) (F _u)	0.005	0.215	0.238	0.246
BBB permeability (log BB)	-2.056	-2.184	-1.493	-1.664
CNS permeability (log PS)	-4.675	-3.96	-3.709	-3.362

Table S4: Predicted metabolic fates of remdesivir, EGCG, myricetin and quercetagenin

Properties	Remdesivir	EGCG	Myricetin	Quercetagenin
CYP2D6 substrate	No	No	No	No
CYP3A4 substrate	Yes	No	No	No
CYP1A2 inhibitor	No	No	Yes	Yes
CYP2C19 inhibitor	No	No	No	No
CYP2C9 inhibitor	No	No	No	No
CYP2D6 inhibitor	No	No	No	No
CYP3A4 inhibitor	No	Yes	No	No

Table S5: Predicted excretion routes of remdesivir, EGCG, myricetin and quercetagenin

Properties	Remdesivir	EGCG	Myricetin	Quercetagenin
Total clearance log ml/min/kg	0.198	0.292	0.422	0.307
Renal OCT2 substrate	No	No	No	No